Cortical regions associated with autonomic cardiovascular regulation during lower body negative pressure in humans

Derek S. Kimmerly[1], Deborah D. O'Leary[1], Ravi S. Menon[2], Joseph S. Gati[2] and J. Kevin Shoemaker[1,3]

[1]*Neurovascular Research Laboratory, Faculty of Health Sciences and School of Kinesiology, The University of Western Ontario, London, Ontario, Canada N6A 3K7*
[2]*Advanced Imaging Laboratories, Robarts Research Institute, London, Ontario, Canada N6A 5K8*
[3]*Department of Physiology and Pharmacology, The University of Western Ontario, London, Ontario, Canada N6A 3K7*

The purpose of the present study was to determine the cortical structures involved with integrated baroreceptor-mediated modulation of autonomic cardiovascular function in conscious humans independent of changes in arterial blood pressure. We assessed the brain regions associated with lower body negative pressure (LBNP)-induced baroreflex control using functional magnetic resonance imaging with blood oxygen level-dependent (BOLD) contrast in eight healthy male volunteer subjects. The levels of LBNP administered were 5, 15 and 35 mmHg. Heart rate (HR; representing the cardiovascular response) and LBNP (representing the baroreceptor activation level) were simultaneously monitored during the scanning period. In addition, estimated central venous pressure (CVP), arterial blood pressure (ABP) and muscle sympathetic nerve activity were recorded on a separate session. Random effects analyses (SPM2) were used to evaluate significant ($P < 0.05$) BOLD signal changes that correlated separately with both LBNP and HR (15- and 35-mmHg *versus* 5-mmHg LBNP). Compared to baseline, steady-state LBNP at 15 and 35 mmHg decreased CVP (from 7 ± 1 to 5 ± 1 and 4 ± 1 mmHg, respectively) and increased MSNA (from 12 ± 1 to 23 ± 3 and 36 ± 4 bursts min^{-1}, respectively, both $P < 0.05$ *versus* baseline). Furthermore, steady-state LBNP elevated HR from 54 ± 2 beats min^{-1} at baseline to 64 ± 2 beats min^{-1} at 35-mmHg suction. Both mean arterial and pulse pressure were not different between rest and any level of LBNP. Cortical regions demonstrating increased activity that correlated with higher HR and greater LBNP included the right superior posterior insula, frontoparietal cortex and the left cerebellum. Conversely, using the identical statistical paradigm, bilateral anterior insular cortices, the right anterior cingulate, orbitofrontal cortex, amygdala, midbrain and mediodorsal nucleus of the thalamus showed decreased neural activation. These data corroborate previous investigations highlighting the involved roles of the insula, anterior cingulate cortex and amygdala in central autonomic cardiovascular control. In addition, we have provided the first evidence for the identification of the cortical network involved specifically with baroreflex-mediated autonomic cardiovascular function in conscious humans.

(Received 27 May 2005; accepted after revision 1 September 2005; first published online 8 September 2005)
Corresponding author J. K. Shoemaker: Neurovascular Research Laboratory, Faculty of Health Sciences and School of Kinesiology, Thames Hall, Room 3110, The University of Western Ontario, London, Ontario, Canada N6A 3K7. Email: kshoemak@uwo.ca

Electrophysiological, neuroanatomical, chemical and electrical stimulation studies have provided an abundance of information regarding the identification of brainstem and cortical sites associated with the modulation of cardiovascular function (Cechetto & Saper, 1990; Dampney, 1994; Verberne & Owens, 1998). Although it has been well established that the medulla oblongata is the primary autonomic cardiovascular control centre, recent studies have highlighted the importance of certain forebrain structures involved with the modulation of efferent autonomic outflow. A major system involving cardiovascular regulation is the neuronal network that encompasses the baroreflex including peripheral receptors in the cardiac chambers, aorta and carotid sinus, medullary relay nuclei, and the efferent signals to the heart and vasculature. In addition, specific cortical regions associated with baroreceptor-mediated cardiovascular function include the insular cortex (Butcher & Cechetto, 1995; Zhang *et al.* 1999), anterior cingulate cortex (ACC) (Terreberry & Neafsey, 1987; Verberne & Owens,

 DOI: 10.1113/jphysiol.2005.091637

1998), amygdala (Cechetto & Calaresu, 1983, 1984, 1985; Gelsema *et al.* 1989) and the cerebellum (Bradley *et al.* 1987*b*; Nisimaru *et al.* 1998). There have been a limited number of cortical stimulation experiments performed in humans. Electrical stimulation of the insula (Oppenheimer *et al.* 1992), anterior cingulate cortex (Pool & Ransohoff, 1949) and the medial temporal lobe (Fish *et al.* 1993) have all demonstrated changes in both blood pressure and heart rate (HR). Additionally, functional magnetic resonance imaging (fMRI) investigations have allowed for the non-invasive assessment of cortical autonomic correlates in conscious humans (King *et al.* 1999; Critchley *et al.* 2000; Harper *et al.* 2000; Henderson *et al.* 2002). These experiments have helped to identify the cerebral components of a central autonomic network in humans that include many of the same cortical structures exposed in animal studies. The physiological adaptations characterized by real or simulated orthostatic stress include a reduction in venous return and cardiac filling pressure, followed by baroreceptor-mediated elevations in HR and muscle sympathetic nerve activity (MSNA) allowing for the homeostatic maintenance of arterial blood pressure. Although previous research has elucidated the higher brain regions involved with autonomic cardiovascular control, the cortical structures related to baroreceptor regulation of efferent autonomic outflow are poorly understood in humans. As insightful as the above-mentioned neuroimaging investigations have been, the majority have utilized volitional multiple system approaches (i.e. exercise and mental stress) or pharmacological techniques that ultimately produce large elevations in arterial pressure (King *et al.* 1999; Critchley *et al.* 2000; Harper *et al.* 2000; Henderson *et al.* 2004). The use of such complex manoeuvres makes it difficult to distinguish cortical activity specific to baroreflex function, as opposed to afferent information, from active skeletal muscle or from other cortical areas involved with cognition, memory or emotion. Additionally, the large fluctuations in arterial blood pressure produced by these stressors confound the ability to separate cortical activity associated with baroreflex afferent (i.e. arterial pressure) versus efferent (i.e. HR and/or MSNA) responses. The purpose of the present investigation was to determine the brain regions associated with baroreceptor unloading patterns designed to elicit sympathetic nerve responses alone versus combined sympathetic nerve and HR responses using mild to moderate levels of lower body negative pressure (LBNP). Specifically, changes in HR and the magnitude of baroreceptor unloading during acute central hypovolaemia were examined within a background where the feedback contributions on higher autonomic centres produced by changes in arterial blood pressure and volitional effort were minimized. To our knowledge, this study provides the first evidence highlighting the central cortical network involved in the modulation of autonomic cardiovascular control during physiological orthostatic stress in conscious humans.

Methods

Participants

Eight healthy normotensive (blood pressure, 130/68 mmHg) male participants (24 ± 2 years, 79 ± 6 kg, mean $\pm$ S.D.) were recruited, given a medical screening and completed a magnetic resonance imaging preliminary questionnaire to ensure safe compatibility within a high magnetic field environment. All participants were instructed to refrain from caffeine and alcohol for a minimum of 24 h, and intense physical exertion at least 12 h, prior to their first test session. Previously, we reported that hypovolaemia increases MSNA at rest and during orthostatic stress (Kimmerly & Shoemaker, 2002). Therefore, participants were instructed to ingest 250 ml water every hour beginning ~6 h prior to sleep the night before and during the morning of each test. With the exception of volume loading, all participants arrived to the laboratory after a 12-h fast. All participants were asked to void their bladder before instrumentation to minimize the effects of a distended bladder on sympathetic activity and arterial blood pressure (Fagius & Karhuvaara, 1989). Subjects had no history of autonomic dysfunction or cardiovascular disease, and were not on any medications known to affect brain function or perfusion. Following assessment of the study methods and information, subjects provided written consent to participate in this study, which was approved by the University of Western Ontario Review Board for Health Sciences Involving Human Subjects. After each neuroimaging session, subjects were debriefed by asking them about their experience. This provided us with a qualitative determination of the amount of subjective stress experienced during the scanning periods. None of the participants in this study reported feeling any significant degree of aversive emotional stress during the fMRI experiments. Six of the eight participants had participated in similar functional neuroimaging studies prior to the current investigation. During each scanning session, participants were instructed to keep their eyes closed and to avoid quick and excessive head movements.

Experimental design

The subjects participated in two separate experimental sessions: the physiological recording session performed at the Neurovascular Research Laboratory and the fMRI session performed at Robarts Research Institute. The session order was randomly assigned but performed at the same time of day and separated by a minimum

period of 1 week. Subjects were familiarized with the experimental procedures prior to their first test session. Each session began with the subject in the supine position and sealed within the LBNP chamber for a minimum of 30 min. Three levels of randomly assigned LBNP (5, 15 and 35 mmHg) were used in the present investigation. The 5-mmHg level of LBNP was the control session, performed to simulate the subjective sensory and emotional experience associated with the neuroimaging sessions (i.e. auditory sensations) without producing a significant amount of cardiovascular stress. Subsequently, both the 15- and 35-mmHg functional imaging data were compared against the 5-mmHg sessions in an attempt to minimize confounding influences related to somtatosensory input and therefore enhance our ability to detect signal changes related specifically to baroreceptor unloading. Within each session, subjects were exposed to four 45-s bouts of LBNP with a 30-s rest period between each repetition. For each subject, the same order of LBNP application was replicated for each test session. All eight participants performed the initial fMRI session, forming the 'Main' group. In addition, six of the eight subjects participated in a repeat fMRI session performed at the same time of day and using the identical LBNP order as their previous fMRI recording session (the 'Repeat' group).

To simulate physiological orthostasis during the fMRI recording sessions, a specially designed LBNP chamber was constructed to fit within the bore of the scanner. To control for movement, the combination of MAST antishock trousers (David Clark Company Inc., Worcester, MA, USA) (Halliwill *et al.* 1998), a non-ferromagnetic height adjustable bicycle seat and a footplate were built into the chamber. Using the MAST trousers, the subject was no longer under the cardiovascular stress of lower body suction when the pants were inflated. This system was capable of minimizing subject movement to ∼1 mm within a given recording session. Sessions in which subject movement was greater than 1 mm were not used for data analysis. A total of three individual LBNP trials in the Main group during 35-mmHg LBNP (total trials, 32) were excluded from data analysis. Prior pilot testing comparing the estimated central venous pressure (CVP) response without (Fig. 1*A* and *B*) and with (Fig. 1*C* and *D*) the use of the antishock trousers indicated that trouser inflation did not significantly affect cardiac filling parameters during LBNP.

Physiological recording session

Data acquisition. HR was monitored from a standard three-lead ECG. Arterial blood pressure (ABP) was measured continuously from the finger of the left hand by photoplethysmographic methods (model 2300 Finapres, Ohmeda; Englewood, CA, USA) (Parati *et al.* 1989). The blood pressures recorded from the Finapres device were corrected against sphygmomanometrically

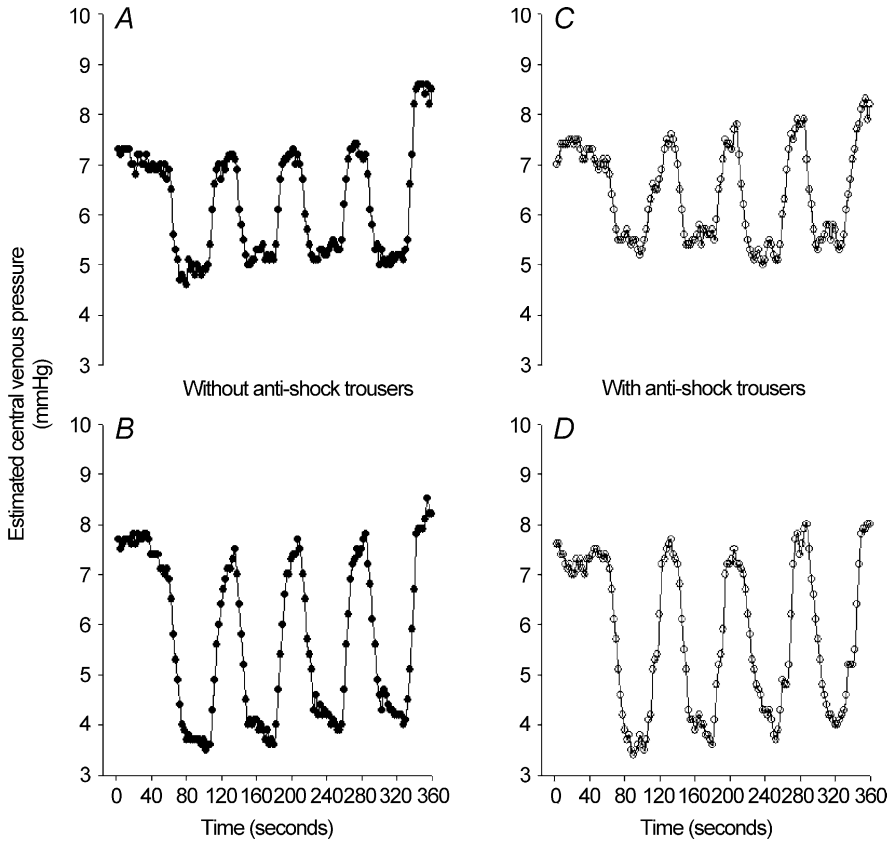

Figure 1. The effect of antishock trousers on changes in estimated central venous pressure during LBNP
Individual data averaged into 2.5-s bins highlighting the similarity in the magnitude and the time course response of estimated central venous pressure during application of 15-mmHg LBNP (*A* and *C*) and 35-mmHg LBNP (*B* and *D*).

obtained systolic and diastolic pressures that were made intermittently during data collection. CVP was estimated from antecubital venous pressure in the dependent right arm referenced to heart level.

Multi-fibre recordings of sympathetic activity were assessed using microneurographic techniques (Hagbarth & Vallbo, 1968; Delius *et al.* 1972) from the common peroneal nerve, as used previously in our laboratory (Kimmerly & Shoemaker, 2002; Kimmerly *et al.* 2004).

Data analysis. Analog signals for ABP, CVP and MSNA were sampled at 200 Hz, and at 400 Hz for ECG, and collected with an on-line data acquisition and analysis system (PowerLab, ADInstruments, Castle Hill, NSW, Australia). Pulse pressure (PP) was calculated as systolic minus diastolic pressure and mean arterial pressure (MAP) was calculated as diastolic pressure plus one-third of PP.

Only pulse-synchronous bursts of MSNA activity with characteristic rising and falling slopes, and amplitudes that were at least twice that of the interburst baseline fluctuations (2 : 1 signal/noise), were included in the analysis. MSNA was measured for frequency (bursts min^{-1}) during each baseline period and LBNP level.

Neuroimaging recording session

fMRI data acquisition. During the scanning session, HR was calculated from the pulse intervals recorded on an MRI-compatible Oximeter (Nonin Medical Inc, 8600FO MRI, Plymouth, MN, USA) placed over the middle finger of the left hand. The absolute level of LBNP was simultaneously measured during each scanning session with the use of a pressure transducer (Edwards Lifesciences, PX272, Irvine, CA, USA) connected in series to a bridge amplifier outside the MRI suite.

All imaging data were collected on a whole body 4-Tesla imaging system (Varian, Palo Alto, CA, USA; Siemans, Erlangen, Germany) with a maximum strength of $40\ \mathrm{mT\,m^{-1}}$ and a slew rate of $120\ \mathrm{mT\,m^{-1}\,s^{-1}}$. A transmit–receive cylindrical hybrid birdcage radio frequency (RF) head coil (Barberi *et al.* 2000) was used for transmission and detection of the blood oxygen level-dependent (BOLD) contrast signal. Prior to imaging, a global shimming procedure (RASTAMAP) using first- and second-order shims, was performed to optimize the magnetic field over the imaging volume of interest (Klassen & Menon, 2004). Twenty-one interleaved contiguous axial slices (5 mm thick, 3 mm × 3 mm in-plane voxel resolution) beginning at the superior end of the cerebral cortices, were acquired in each volume and prescribed from a series of high-resolution T1-weighted sagittal scout images, where T1-weighted refers to images based on a tissue-dependent recovery of the longitudinal component of net magnetization over time. Volume acquisition time (i.e. 21 axial slices) was 2.5 s with a time to repetition (TR) of 0.6250 s (four shots). A total of 133 volumes were collected per session. Five steady-state volumes were acquired prior to actual data collection to allow for magnetization equilibrium; these were discarded prior to data analysis. Functional data were collected using a segmented T2*-weighted gradient echo – echo planar imaging (EPI) pulse sequence (echo time (TE), 12 ms; Flip angle, 45 deg; field of view (FOV), 192 mm × 192 mm) with navigator echo correction. A corresponding high-resolution T1-weighted structural volume was acquired at the beginning of the same scanning session using three-dimensional Turbo FLASH (TE, 5.5 ms; inversion time (TI), 600 ms, TR, 10 ms) with a voxel resolution of 0.75 mm × 0.75 mm × 2.5 mm. Each subject was immobilized during the experimental session within a head cradle that was packed with foam padding, and was instructed to keep their eyes closed and avoid head movements during the scanning period.

fMRI data analysis. The HR and LBNP data were averaged over 2.5-s bins and time aligned to ensure a corresponding mean value for each functional scan (i.e. 133 data points) obtained during the fMRI collection period. All fMRI data were analysed with statistical parametric mapping (SPM2, Wellcome Department of Cognitive Neurology) implemented in Matlab (Mathworks, Sherborn, MA, USA). The images collected during each LBNP session were realigned to the first scan of that session. Realignment was performed using a fourth degree B-spline reslice interpolation method and was used to create a mean EPI image, which was coregistered to the participants' T_1-weighted anatomical image. The origin (e.g. $x,y,z = 0,0,0$ mm) was set at the anterior commissure (AC) parallel to the AC– posterior commissure (PC) line. All volumes were then transformed into a canonical stereotactic space (International Consortium for Brain Mapping (ICBM), National Institutes of Health P-20 project; template image, avg152T1.mnc) using a trilinear interpolation method and a bounding box with dimensions: x, −90 : 90 cm, y, −126 : 90 cm and z, −72 : 108 cm.

For optimal coregistration with this structural template, the anatomical image was bias-corrected (extremely light) and non-linearly normalized (very heavy regularization) with a resampled voxel size of 2 mm × 2 mm × 2 mm. To correct for resultant errors from fixed deterministic drifts, a high-pass filter (cut-off period, 150 s) was applied to all functional images. The scans were smoothed using a Gaussian kernel set at 8-mm full width at half-maximum (FWHM).

Statistical analysis

The main effects of recording session (neuroimaging *versus* physiological) or group (i.e. Main *versus* Repeat) and level

Table 1. Selected haemodynamic and sympathetic nerve data during supine rest (baseline) and steady-state LBNP

Condition	HR (MRI) (beats min^{-1})	HR (LAB) (beats min^{-1})	PP (LAB) (mmHg)	MAP (LAB) (mmHg)	CVP (LAB) (mmHg)	MSNA (LAB) (bursts min^{-1})
Baseline	57 ± 2	56 ± 2	62 ± 3	89 ± 3	7.4 ± 1.1	12 ± 3
5 mmHg	55 ± 1	55 ± 2	61 ± 3	86 ± 2	7.0 ± 0.8	16 ± 3
15 mmHg	55 ± 2	56 ± 1	61 ± 4	86 ± 4	5.2 ± 0.9*	23 ± 2*
35 mmHg	64 ± 2*	64 ± 3*	59 ± 3	91 ± 4	3.7 ± 1.0*	36 ± 4*

Data are means ± S.E.M. MRI represents data collected during the neuroimaging test session; LAB, represents data collected during the physiological recording test session. HR, heart rate; PP, pulse pressure; MAP, mean arterial pressure; CVP, estimated central venous pressure; MSNA, muscle sympathetic nerve activity. *Significant difference ($P < 0.05$) from baseline.

of LBNP on HR were analysed using a repeated-measures two-way ANOVA. All other haemodynamic and MSNA variables collected during the physiological test session only were analysed using a one-way ANOVA with repeated measures. When significant main effects were observed, Tukey's *post hoc* analysis was performed to estimate differences among means. Probability levels during multiple point-wise comparisons were corrected using Bonferonni's approach. Statistical significance in all comparisons was set at $P < 0.05$. Values are presented as means ± S.E.M.

A two-level statistical protocol was used for all functional imaging data. Firstly, individual design matrices were constructed for the analysis of participant-by-session interactions to determine cortical areas where BOLD activity covaried (bi-directionally) with HR and LBNP separately. This created a participant-by-session contrast image for each subject at each level of LBNP. These contrast images were taken to a second level of statistical analysis where paired *t* tests were performed to determine the brain regions that demonstrated more or less activation during 15- and 35-mmHg LBNP *versus* 5-mmHg LBNP. The use of LBNP and HR, as physiological regressors to the BOLD signal, allowed for the representation of the input and output components of baroreceptor function, respectively. To account for potential variations in global BOLD signal caused by lower body suction, all images were intensity normalized so that relative signal changes within each scan could be determined.

In additional to a global analysis of forebrain responses, specific regions of interest (ROI) were isolated statistically for more detailed analysis. The ROI were selected based on previous animal and human data related to cortical structures implicated in central autonomic cardiovascular regulation. In human stimulation (Pool & Ransohoff, 1949; Oppenheimer *et al.* 1992) and functional imaging (Williamson *et al.* 1997; Fredrikson *et al.* 1998; Soufer *et al.* 1998; Williamson *et al.* 2004) studies, ACC and insula have been associated with central autonomic control. Lesion studies in humans have highlighted the potential role of the prefrontal/orbitofrontal cortex (Tranel & Damasio, 1994) and the amygdalo-hippocampal complex (Bechara *et al.* 1995) in sympathetically mediated cardiovascular regulation. In addition, many animal studies have implicated the cerebellum (Bradley *et al.* 1987*a*,*b*), primary somatomotor cortices (Cechetto & Saper, 1990) and brainstem (Cechetto & Saper, 1990; Spyer, 1999) in central cardiovascular function. All masks were generated using the WFU_PickAtlas program (version 1.04) (Maldjian *et al.* 2003).

To minimize the impact of a type II error, the significance level for these *a priori* regions of interest were set at $P < 0.001$, uncorrected for multiple comparisons over the entire brain volume. Paired *t* test significance levels were set at $P < 0.05$, small volume corrected. Significant local maximal voxel coordinates are reported in both Montreal Neurological Institute (MNI) and Talairach (TAL) formats. Non-linear transformations from MNI to TAL were calculated using a specialized Matlab function. In addition, neuroanatomical localization and determination of Brodmann areas were performed using the Talairach Daemon software (Lancaster *et al.* 2000). All brain region coordinates reported in the current study were common to the random effects analyses for both the Main ($n = 8$) and Repeat ($n = 6$) groups separately. Significant results are only reported for cluster sizes equal to or greater than 10 voxels. All fMRI figures are represented in a neurological convention (i.e. participant's left is on the left).

Results

There were no between-trial differences ($P > 0.3$, all comparisons) for any of the three LBNP sessions (MRI or laboratory) for any haemodynamic or MSNA variables. Therefore, the average steady-state data (i.e. the last 30 s of each replicated LBNP exposure) of the four within-session trials are reported.

Physiological data

Average steady-state HR, MAP and CVP data collected during the physiological and neuroimaging recording sessions were not different (Table 1). Furthermore, the

baseline and steady-state LBNP heart rate data collected during the repeat neuroimaging session ($n = 6$) were not different ($P > 0.32$, all comparisons) from those observed in the main group ($n = 8$). Group-averaged time course responses of HR and LBNP are displayed in Fig. 2. For purposes of clarity, the s.e.m. bars were omitted from the graph. The largest s.e.m. for any single 2.5-s averaged data point was 3.1 beats min^{-1} and 1.5 mmHg for HR and LBNP data, respectively. There were no differences ($P > 0.11$) in arterial pulse or mean (Table 1) blood pressures between baseline and any level of LBNP. Central venous pressure was unchanged ($P > 0.46$) with 5-mmHg LBNP (−0.4 mmHg). However, there was a significant reduction in CVP during 15- (−1.9 mmHg) and 35-mmHg LBNP (−3.6 mmHg) ($P < 0.02$, for both).

The steady-state MSNA burst frequency data during baseline and LBNP are presented in Table 1. No significant LBNP-induced increase in burst frequency was observed during 5-mmHg LBNP. Conversely, burst frequency was augmented with 15-mmHg LBNP (11 bursts min^{-1}; $P < 0.01$) and 35-mmHg LBNP (25 bursts min^{-1}; $P < 0.001$).

Functional MRI data

To characterize the dynamic relationship between cortical neural activity and the physiological covariates (HR and LBNP), we performed bi-directional regression analyses. Central neural structures that showed augmented BOLD signal at higher HR and/or larger magnitudes of LBNP (i.e. greater baroreceptor unloading) were labelled as having 'increased activation'. Conversely, the term 'decreased activation' denoted those cortical regions that had a relatively attenuated BOLD signal during the same time periods. Furthermore, brain regions demonstrating decreased activation during baroreceptor unloading (or at higher HRs) may also be interpreted as producing greater neural activity during baroreceptor reloading (or at lower HRs). Increased and decreased activation (15- and 35-mmHg LBNP *versus* 5-mmHg LBNP) data of brain sites correlated with LBNP and HR are displayed in Tables 2–5. Each table indicates the cortical region, Brodmann area (BA), side and size (in voxels) of the associated brain area, MNI and TAL coordinates, and T and Z-scores. All brain areas represented in these tables were implicated in

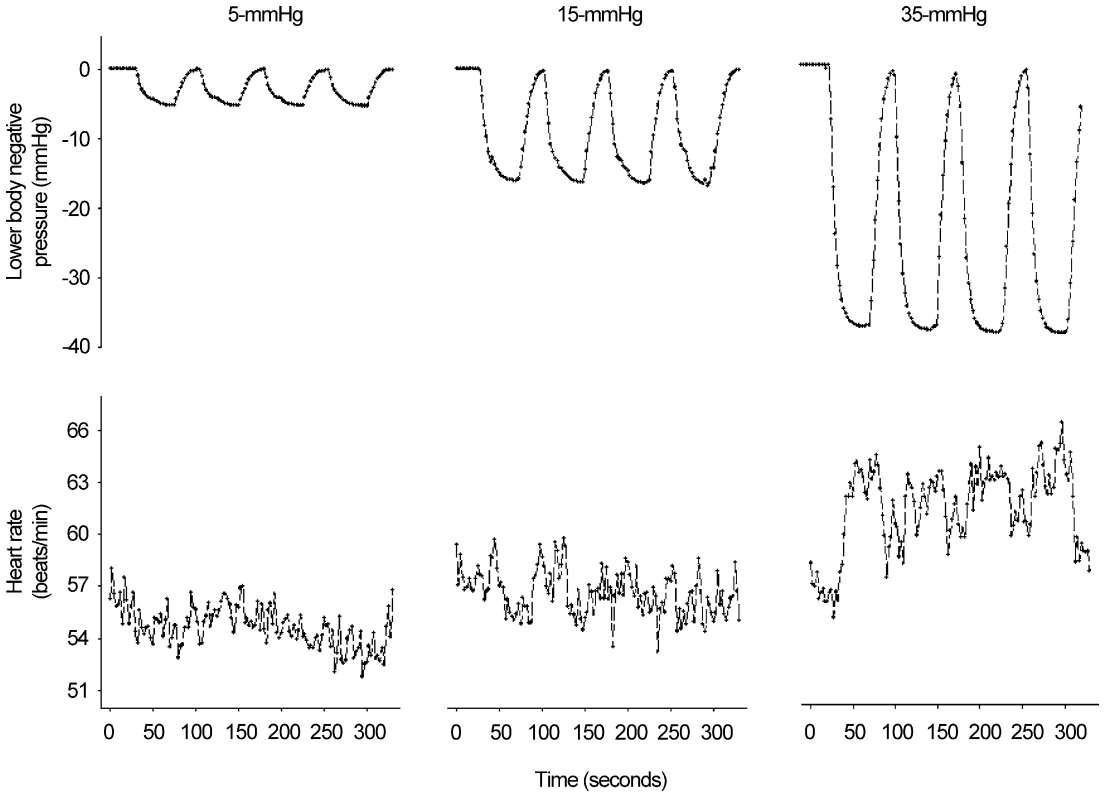

Figure 2. Group average LBNP and heart rate data used to correlate with fMRI-BOLD signal
LBNP and HR data were averaged every 2.5 s corresponding to each volume (133 total) of fMRI-BOLD data acquired during the scanning session.

Table 2. Brain regions covarying with mild lower body negative pressure (15 > 5-mmHg) common to both the Main ($n = 8$) and Repeat ($n = 6$) groups

Location (Brodmann area)	Side	MNI (*x*, *y*, *z*)	TAL (*x*, *y*, *z*)	Voxels (no.)	T-score	Z-score
A. Increased activation during baroreceptor unloading						
Middle frontal gyrus (46)	L	− 42, 36, 20	−42, 36, 17	10	3.27	2.74
Middle frontal gyrus (6)	R	44, 0, 54	44, 3, 50	16	3.92	2.98
Inferior frontal gyrus (9)	R	52, 18, 28	52, 19, 25	65	3.89	2.97
Postcentral gyrus (7)	R	6, −54, 70	6, −49, 67	53	4.17	3.10
Precuneus (7)	R	6, −78, 52	5, −73, 52	50	3.51	2.92
B. Decreased activation during baroreceptor unloading						
Insula (13)	L	−40, 12, −6	−42, 12, −3	76	2.63	2.33
	L	−46, 12, 10	−46, 12, 8	96	2.54	2.27
Insula (13)	R	32, 28, 20	32, 26, 20	59	3.42	2.86
Anterior cingulate (32)	R	18, 46, 10	18, 45, 7	10	3.35	3.13
Anterior cingulate (32)	L	− 8, 24, 24	−8, 24, 21	33	3.30	2.79
Orbitofrontal (11)	R	44, 48, −12	44, 46, −12	16	3.33	2.81

MNI, Montreal Neurological Institute co-ordinates; TAL, Talaraich co-ordinates; L, left; R, right.

Table 3. Brain regions covarying with heart rate during mild LBNP (15 > 5-mmHg) common to both the Main ($n = 8$) and Repeat ($n = 6$) groups

Location (Brodmann area)	Side	MNI (*x*, *y*, *z*)	TAL (*x*, *y*, *z*)	Voxels (no.)	T-score	Z-score
A. Increased activation during higher heart rates						
Insula (13)	R	34, −22, 13	34, −21, 13	22	3.08	2.53
Precentral gyrus (6)	R	40, −12, 34	40, −10, 32	12	2.89	2.41
Postcentral gyrus (3)	R	44, −22, 60	44, −19, 56	17	3.05	2.63
Cerebellum	L	−14, −52, −25	−14, −51, −18	23	2.87	2.39
B. Decreased activation during higher heart rates						
Anterior cingulate (32)	R	18, 46, 12	18, 45, 9	54	3.05	2.69
Amygdala	L	−22, 0, −26	−22, −1, −22	14	2.86	2.39
Thalamus (medial dorsal nucleus)	L	−12, −20, 12	−12, −19, 12	12	3.00	2.80

MNI, Montreal Neurological Institute co-ordinates; TAL, Talaraich co-ordinates; L, left; R, right.

both the Main and Repeat group random effects statistical analyses ($P < 0.05$, corrected).

Cerebral correlates associated with mild (15-mmHg *versus* 5-mmHg) LBNP

Correlates with LBNP. Central neural structures that displayed increased BOLD signal during 15-mmHg LBNP (*versus* 5-mmHg LBNP) included the left (BA 46) and right (BA 6) middle frontal gyrus, right inferior frontal (BA 9) and postcentral (BA 7) gyri along with the right precuneus (BA 7) (Table 2*A*). Right orbitofrontal (BA 11), bilateral insula (BA 13) and anterior cingulate (BA 32) cortical regions showed decreased neural activity at 15-mmHg of LBNP (Table 2*B*).

Correlates with heart rate. Brain sites that showed increased neural activation associated with higher HR common to 15-mmHg LBNP included the right posterior insula (BA 13), right precentral gyrus (BA 6), right postcentral gyrus (BA 3) and a small region of the left cerebellar hemisphere (Table 3*A*). The left amygdala, right anterior cingulate (BA 32) and left mediodorsal thalamus demonstrated decreased activation at higher HR during 15-mmHg LBNP (Table 3*B*).

Cerebral correlates associated with moderate (35-mmHg *versus* 5-mmHg) LBNP

Correlates with LBNP. Cortical regions covarying with the magnitude of lower body negative pressure during 35-mmHg LBNP that were also observed during 15-mmHg LBNP included the left (BA 46) and right (BA 6) middle frontal gyrus, right inferior frontal (BA 9) and postcentral (BA 7) gyri along with the right precuneus (BA 7) (Table 4*A*). In addition, the right insula (BA 13), right superior frontal (BA 10) and left precentral (BA 6) gyri also demonstrated an increase in signal intensity during the 35-mmHg LBNP (Table 4*A*, Fig. 3*A* and *B*). Furthermore, a paired *t* test demonstrated greater activity in the right middle frontal gyrus (BA 6) during 35-mmHg *versus* 15-mmHg LBNP sessions. Similarly, all the cerebral centres demonstrating decreased activation related to the degree of baroreceptor unloading in the 15-mmHg LBNP session were also represented during the moderate level of orthostatic stress (Table 4*B* and Fig. 3*D*). In addition to

Table 4. Brain regions covarying with moderate lower body negative pressure (35 > 5-mmHg) common to both the Main ($n = 8$) and Repeat ($n = 6$) groups

Location (Brodmann area)	Side	MNI (*x*, *y*, *z*)	TAL (*x*, *y*, *z*)	Voxels (no.)	T-score	Z-score
A. Increased activation during baroreceptor unloading						
Insula (13)	R	46, 0, 0	40, 0, 0	71	4.58	3.52
Superior frontal gyrus (10)	R	30, 54, 0	30, 52, −3	12	4.31	3.38
Middle frontal gyrus (46)	L	−42, 38, 24	−42, 38, 20	80	5.32	3.87
Middle frontal gyrus (6)	R	48, 4, 50	48, 6, 46	28	4.35	3.41
Inferior frontal gyrus (9)	R	58, 20, 26	58, 21, 23	58	4.44	2.85
Precentral gyrus (6)	L	−60, −16, 42	−60, −14, 40	22	4.83	3.64
Postcentral gyrus (7)	R	8, −58, 68	8, −53, 65	19	3.97	3.19
Precuneus (7)	R	5, −78, 50	5, −73, 50	80	5.04	3.04
B. Decreased activation during baroreceptor unloading						
Insula (13)	L	−38, 14, −6	−38, 13, −6	48	2.23	2.00
Insula (13)	R	30, 22, 12	30, 22, 10	31	8.85	3.85
Anterior cingulate (10)	R	16, 54, 6	16, 52, 3	15	4.60	3.53
Cingulate (31)	R	13, −46, 30	13, −43, 30	73	7.34	4.63
Amygdala	L	−26, −2, −18	−26, −3, −15	41	4.34	3.40
Thalamus (medial dorsal nucleus)	R	6, −14, 14	6, −13, 13	19	4.46	3.46
Orbitofrontal (11)	R	46, 44, −10	46, 42, −11	24	3.89	3.15

MNI, Montreal Neurological Institute co-ordinates; TAL, Talaraich co-ordinates; L, left; R, right.

these brain areas, the right cingulate gyrus (BA 31), left amygdala and right mediodorsal nucleus of the thalamus also displayed decreased BOLD signal during 35-mmHg LBNP (Table 4*B*). Only the region of the left anterior insula showed reduced activation during 35-mmHg *versus* 15-mmHg LBNP.

Correlates with HR. Regions associated with increased activation correlated with higher HR during 15-mmHg LBNP that were also implicated during the 35-mmHg session included: the right posterior inferior insular cortex (BA 13), the right precentral gyrus (BA 6), the right postcentral gyrus (BA 3) and a portion of the left cerebellar hemisphere (Table 5*A* and Fig. 4*A* and *B*). Furthermore, both the right posterior insula and right precentral gyrus demonstrated greater activation during 35-mmHg *versus* 15-mmHg LBNP ($P < 0.05$, small volume corrected). Other cortical areas involved with greater activation at high HR during 35-mmHg LBNP were the right superior frontal gyrus (BA 10) and left middle frontal gyrus (BA 6) (Table 5*A*). In addition to the three central structures associated with decreased activity at higher HR during 15-mmHg LBNP (Table 3*B*), the right posterior inferior insula (BA 13; Fig. 4*C*), right amygdala and right midbrain also displayed decreased BOLD activity during 35-mmHg LBNP (Table 5*B*).

Discussion

This study reports the first known representation of the cortical network involved with baroreceptor-mediated autonomic regulation of cardiovascular function induced by transient reductions in central blood volume in humans. It is important to note that both increases and decreases in cortical neural activity were observed during repeated neuroimaging sessions. Moreover, we have shown previously the reproducibility of sympathetic and cardiovascular responses to repeated orthostatic tests separated by several weeks (Kimmerly *et al.* 2004). Therefore, the current findings indicate that when baroreceptor afferent information was reduced, forebrain activity was increased in the right superior posterior insula, left cerebellar hemisphere and specific regions within the frontal and parietal cortices. Conversely, a cortical network including bilateral anterior insula, the right anterior cingulate, amygdala, midbrain and mediodorsal thalamus displayed decreased activation. Thus, under baseline conditions, the latter group of sites appears to be tonically activated to some extent. These data highlight the functional organization of the cerebral cortex mediating baroreceptor reflex-induced control of autonomic cardiovascular function in conscious humans. Moreover, these central neural responses were observed without concurrent changes in mean arterial or peripheral pulse pressures thus minimizing the feedback contributions of these physiological inputs on arterial baroreceptor-mediated central autonomic regulation.

Cortical regions demonstrating increased neural activation to baroreceptor unloading

In addition to projections through brainstem nuclei, there are reciprocal connections between cortical regions and the nucleus tractus solitarius (NTS) and rostral ventrolateral medulla (RVLM) mediating baroreflex cardiovascular function (Cechetto & Saper, 1990; Verberne

Table 5. Brain regions covarying with heart rate during moderate LBNP (35 > 5-mmHg) common to both the Main ($n = 8$) and Repeat ($n = 6$) groups

Location (Brodmann area)	Side	MNI (*x*, *y*, *z*)	TAL (*x*, *y*, *z*)	Voxels (no.)	T-score	Z-score
A. Increased activation during higher heart rates						
Insula (13)	R	36, −34, 18	34, −32, 18	46	3.95	2.56
Superior frontal gyrus (10)	R	22, 60, 16	22, 59, 12	15	3.95	3.18
Middle frontal gyrus (6)	L	−8, −6, 46	−8, −4, 43	48	4.15	3.30
Precentral gyrus (6)	R	46, −6, 54	46, −3, 50	16	3.59	2.97
Postcentral gyrus (3)	R	44, −18, 56	44, −15, 52	16	4.31	2.80
Cerebellum	L	−28, −50, −36	−28, −50, −28	17	4.25	3.35
B. Decreased activation during higher heart rates						
Insula (13)	R	44, −8, −2	44, −8, −1	116	3.83	3.11
Anterior cingulate (32)	R	4, 44, 2	4, 43, 0	132	4.16	3.30
Amygdala	L	−22, −6, −20	−22, −3, −21	133	3.66	3.01
Amygdala	R	26, −2, −26	26, −3, −21	15	3.84	3.12
Thalamus (medial dorsal nucleus)	L	−6, −16, 12	−6, −15, 12	39	4.37	2.82
Midbrain	R	2, −32, −14	2, −32, −10	22	7.08	3.54

MNI, Montreal Neurological Institute co-ordinates; TAL, Talaraich co-ordinates; L, left; R, right

& Owens, 1998). In the current study, a reproducible autonomic network of central structures was observed that showed increased neural activity during baroreceptor unloading. Specific regions included the right insular cortex, the cerebellum and a few localized regions within the frontal and parietal cortices (Tables 2*A*, 3*A*, 4*A* and 5*A*). This pattern of change was observed during both 15- and 35-mmHg LBNP when MSNA was elevated. Therefore, it

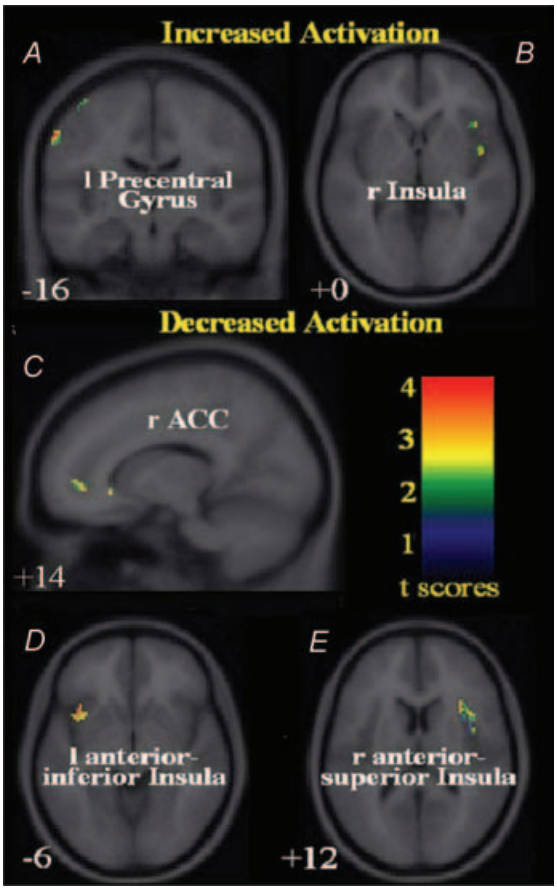

Figure 3. Brain regions associated with changes in LBNP
Increased (*A*–*C*) and decreased (*D* and *E*) activation correlated with LBNP (35-mmHg LBNP > 5-mmHg LBNP).

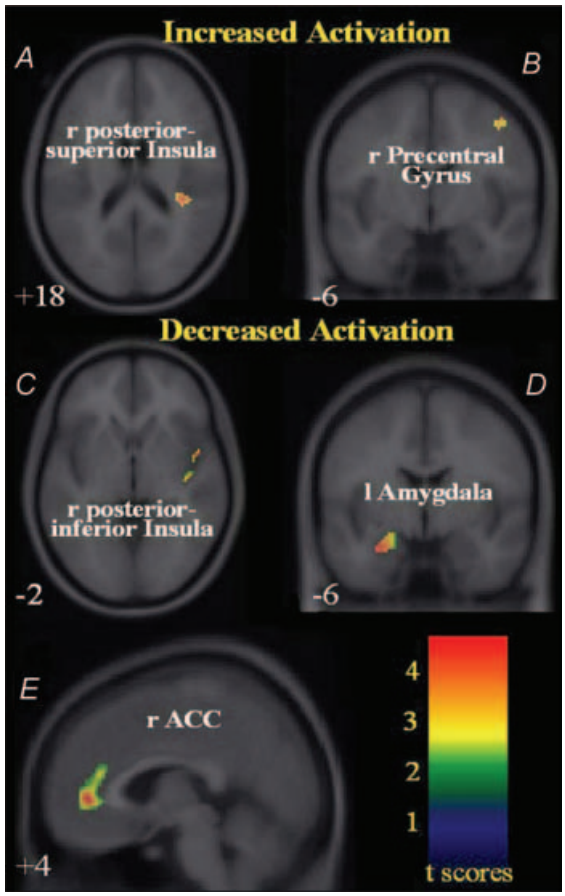

Figure 4. Brain regions associated with changes in heart rate
Increased (*A*–*C*) and decreased (*D* and *E*) activation correlated with heart rate (35-mmHg LBNP > 5-mmHg LBNP).

is tempting to classify these regions as sympatho-excitatory during baroreceptor unloading. However, the possibility exists that these areas accommodate these excitatory responses through a process of disinhibition over other autonomic control sites normally responsible for the constraint of sympathetic outflow. Unfortunately, this interpretational dilemma could not be addressed within the limits of this study.

The right posterior insula is tonically active (Butcher & Cechetto, 1995), contains neurones responsive to baroreceptor input and produces changes in HR and blood pressure upon activation (Zhang & Oppenheimer, 1997). Furthermore, electrophysiological studies during pharmacological blood pressure challenges have repeatedly shown a high percentage of sympatho-excitatiory neurones within the right posterior insula (Oppenheimer & Cechetto, 1990; Zhang & Oppenheimer, 1997; Zhang *et al.* 1998). In the current investigation, the right posterior insular cortex demonstrated both increased and decreased neural activity during baroreceptor unloading (Table 5*A* and *B*). Specifically, the superior portion was associated with increased activation and the inferior region with decreased activation during periods when HR was elevated. These results corroborate the cardiac chronotropic organization of the posterior insula previously described (Oppenheimer & Cechetto, 1990). In this earlier animal model, regions of the posterior insula influencing tachycardia were more superior to those that elicited bradycardia. In addition, both chemical and electrical stimulation of the superior posterior insula elicited pressor effects, whereas depressor responses were observed from more caudal areas suggesting a role for this region in the regulation of efferent sympathetic cardiac function. Therefore, our finding of increased activation within the superior posterior right insula during baroreceptor unloading lends further support to the role of this cortical region in the regulation of efferent sympathetic cardiac and vasomotor function.

The cerebellum is an important component of the central autonomic network and has previously been implicated in the regulation of cardiovascular function during passive head-up tilt in rabbits (Nisimaru *et al.* 1998). Furthermore, bilateral lesions within the cerebellum impaired recovery of MAP after nitroprusside-mediated hypotension (Chen *et al.* 1994). In the current study, a localized region of the left cerebellar hemisphere displayed increased signal intensities associated with HR elevations (Tables 3*A* and 5*A*). Increased activation within a similar region of the left cerebellum has also been associated with increases in HR elicited by mental stress and exercise (Critchley *et al.* 2000). In addition, other neuroimaging experiments have also reported increased cerebellar activation during pharmacologically induced hypotensive challenges (Henderson *et al.* 2002, 2004) and the Valsalva manoeuvre (Henderson *et al.* 2002), emphasizing a role for this brain region in the regulation of cardiovascular function. Therefore, regardless of changes in arterial blood pressure, the cerebellum appears to affect circulatory function via the modulation of efferent autonomic activity. Specifically, the cerebellum can influence autonomic output and modify baroreflex control by augmenting cardiovascular responses mediated by the sympathetic nervous system or by inhibiting those mediated by the parasympathetic nervous system.

Both mild and moderate LBNP elicited increases in neural activity in multiple regions within the frontal and parietal cortices, including the somtatosensory cortex (Tables 2*A* and 4*A*). To our knowledge, this is the first evidence that specific regions within the frontal (BA 6, 9, 10 and 46) and parietal (BA 7) cortices are involved in reflex cardiovascular control. There are a limited number of studies that have focused on the autonomic function of these particular areas of the cerebral cortex. During the Valsalva manoeuvre, Henderson *et al.* (2003) observed an increase in neural activity within similar areas of the frontal cortex as in the current study. Additionally, greater cerebral blood flow (CBF) measured using positron emission tomography (PET), has been observed in the somtatosensory region during exercise (Critchley *et al.* 2003) and mental stress (Critchley *et al.* 2000) related to changes in HR and MAP (Critchley *et al.* 2000), suggesting the involvement of similar regions in the control of central autonomic function.

Cortical regions demonstrating decreased neural activation to baroreceptor unloading

In the current investigation, the primary cortical centres that demonstrated decreased neural activity during integrative baroreceptor unloading included bilateral anterior insula cortices (BA 13), the right anterior cingulate (and medial prefrontal) cortex (BA 10 and 32), the amygdala, the midbrain and the mediodorsal nucleus of the thalamus (Tables 2*B*, 3*B*, 4*B* and 5*B*). This activation pattern would be consistent with that experienced by the baroreceptor afferents (i.e. decreased afferent activity during LBNP), and suggests that these cortical regions could be tonically activated by primary baroreceptor afferent input. Unfortunately, this hypothesis could not be addressed given the limitations of human imaging data. Within the context of previous observations, these results suggest that these cortical areas receive baroreceptor-related information indirectly through medullary relay nuclei (i.e. the NTS) (Verberne & Owens, 1998).

Electrophysiological and neuroanatomical evidence have established reciprocal neural connections between

baroreceptive regions in these structures with cardiovascular centres in the NTS and RVLM (Verberne & Owens, 1998). Furthermore, baroreceptor-related neuronal interconnections have been observed both within and between the above-mentioned cortical structures. Specifically, both the insular cortex and anterior cingulate have direct baroreflex-associated neuronal connections with each other (Verberne & Owens, 1998), and to the amygdala (Yasui *et al.* 1991) and the mediodorsal nucleus of the thalamus (Zhang & Oppenheimer, 2000*a*). The medial prefrontal cortex also sends efferents to the midbrain periaqueductal grey area, which has been shown to influence sympathetic vasomotor activity and circulatory function (Verberne & Owens, 1998). This is consistent with the current observation of synchronized decreased activations of the ACC and midbrain associated with higher HR during integrative baroreceptor unloading (Table 5*B*). Furthermore, electrophysiological evidence has characterized insulo-insular connectivity of baroreceptive neurones in the rat (Zhang & Oppenheimer, 2000*b*). The current functional neuroimaging data lend support to these interconnections as common decreases in neural activity were consistently detected within the anterior insular cortices, anterior cingulate cortex, amygdala and mediodorsal thalamus during baroreceptor unloading (Tables 2*B* and 5*B*).

Both the left and right anterior insular cortices consistently demonstrated decreased neuronal activation during baroreceptor unloading (Tables 2*B* and 4*B*). Therefore, these tonically active regions may be 'listening' to baroreceptor inputs and/or acting as a 'brake' on baseline HR through the involvement of lowering sympathetic or elevating parasympathetic autonomic contributions. During surgical preparations, bilateral stimulation of the anterior insular cortex in humans was associated more with decreases than increases in HR (Oppenheimer *et al.* 1992), suggesting direct control of vagally mediated cardiac function. Therefore, the decreased activation of the anterior insula observed in the present investigation, may affect a withdrawal of cardiac parasympathetic tone during baroreceptor unloading. This earlier study (Oppenheimer *et al.* 1992), also concluded that parasympathetic and sympathetic modulation appears to be lateralized in the insula, with parasympathetic control principally sited on the left side. Additionally, the right anterior insula has been implicated in the awareness of bodily processes and measures of subjective emotional experience (Critchley *et al.* 2004). In a separate neuroimaging study, increased neural activity within the right anterior insula was observed in association with lower HR (Critchley *et al.* 2000). This observation corroborates our finding of decreased neural activity in this region correlated with the magnitude of baroreceptor unloading (Table 4*B*) when HR was elevated. Taken together, these findings suggest that the anterior insular cortex could be involved in baroreceptor-mediated parasympathetic control of cardiovascular function

The anterior cingulate is a large cortical structure located around the rostral portion of the corpus callosum and has frequently been implicated in the modulation of autonomic efferent activity (Verberne & Owens, 1998). The regions defined as the anterior cingulate and orbitofrontal cortex in the present study, are included within the region termed the medial prefrontal cortex (MPFC) by others (Verberne & Owens, 1998; King *et al.* 1999). In the present study, regions of the right anterior cingulate (BA 10 and 32) and orbitofrontal cortex demonstrated decreased neuronal activity associated with baroreceptor unloading and elevated HR during both mild and moderate LBNP (Tables 2*B*, 3*B*, 4*B* and 5*B*). This is in agreement with the results of previous neuroimaging investigations that observed increased activity with similar regions of right ACC (Critchley *et al.* 2000) and orbitofrontal cortex (Weisz *et al.* 2001) associated with increases in arterial pressure or neck chamber-induced baroreceptor stimulation. However, the current results indicate further that regions of the ACC appear to be tonically active at baseline levels of baroreceptor loading in the supine position.

Neurones from the ACC project to subcortical brain regions associated with cardiovascular homeostasis and autonomic control, including the depressor area of the caudal intermediate NTS (Owens & Verberne, 1996). Electrical stimulation of the MPFC in animals elicits hypotension and bradycardia (Buchanan *et al.* 1985) accompanied by sympatho-inhibition of splanchnic and lumbar sympathetic nerve trunks (Verberne & Owens, 1998). In general, the ACC/MPFC contains neurones which, when activated, exert an inhibitory influence on sympathetic vasomotor function. The mechanisms associated with this response probably involve the inhibition of RVLM sympatho-excitatory neurones (Verberne & Owens, 1998). Therefore, the present observation of decreased neuronal activity within this cortical structure during baroreceptor unloading probably represents a disinhibition of sympatho-excitatory pathways facilitating the elevations in both HR and sympathetic vasoconstrictor tone. These data support the view that the prefrontal and orbitofrontal regions play an active role in the processing of information arriving from primary baroreceptor afferents. Furthermore, concurrent reductions in the neural activity of these sympatho-inhibitory regions, together with increased activation of the right superior posterior insula during baroreceptor unloading, could possibly represent an important control network for sympathetically mediated cardiovascular control.

Electrophysiological, chemical stimulation and *c-fos* gene expression investigations have demonstrated that the amygdala is also involved in both reflex and behaviourally

coupled cardiovascular control (Cechetto & Calaresu, 1984; Polson *et al.* 1995). Afferents enter the amygdala from the thalamus and brainstem sites involved in cardiovascular regulation, while efferents from the amygdala project to autonomic control sites in the hypothalamus and brainstem. In the current study, decreased activation was observed in the amygdala associated with higher HR and greater degrees of baroreceptor unloading. Similar to our findings, Critchley *et al.* (2000) observed greater activation of the left amygdala during control conditions than during autonomic stressors associated with increases in blood pressure and HR. Furthermore, in a region of the left amygdala with strikingly similar coordinates to this study, they also found decreased activity in this area associated with elevated HR. This cortical structure may function to restrain efferent sympathetic outflow at rest as neural activity was decreased during periods when MSNA and/or HR were elevated. This is in agreement with the results from previous studies showing that electrical stimulation of the amygdala in rabbits produced bradycardia, hindlimb vasodilatation and hypotension (Dampney, 1994).

Limitations

Since its introduction (Stevens & Lamb, 1965), the LBNP technique has been used to study the circulatory responses to central hypovolaemia in humans. Traditionally, mild LBNP (< 20 mmHg) has been proposed to selectively unload cardiopulmonary baroreceptors and augment peripheral sympathetic nerve activity with minimal change in HR (Zoller *et al.* 1972; Johnson *et al.* 1974). With more severe reductions in central blood volume, a reflex response associated with combined unloading of both cardiopulmonary and arterial baroreceptors is engaged leading to parallel increases in both MSNA and HR. The present study was not designed to identify the specific baroreceptor population responsible for the measured physiological responses, and earlier observations indicate that even 5 mmHg of suction may affect aortic arterial baroreceptor levels (Taylor *et al.* 1995). Thus, while the population of baroreceptors that was affected by the current protocol cannot be determined, the graded LBNP protocol used in this study was successful at eliciting a differential response pattern between 15-mmHg (i.e. increased MSNA) and 35-mmHg (i.e. increased MSNA and HR) LBNP. Consequently, under the current assumptions that 5-mmHg LBNP did not elicit a significant baroreflex stress, contrasting the fMRI data at 15- and 35-mmHg LBNP against 5-mmHg LBNP may have underestimated the cortical population involved with baroreflex-mediated autonomic adjustments. The primary goal of using 5-mmHg LBNP was to mimic the somtatosensory experiences associated with lower body suction and subsequently minimize any related cortical activity at higher LBNP levels. We acknowledge that this low level of LBNP may imperfectly match the stimulus intensity produced with higher degrees of suction. However, with no observable changes in either cardiovascular or sympathetic nerve data, these somtatosensory sensations were probably the predominant source of afferent information modifying cortical activity during 5-mmHg LBNP.

A major difficulty in interpreting our functional neuroimaging data is knowing whether increases in neuronal activity associated with the magnitude of baroreceptor unloading or elevations in HR reflect inhibition of parasympathetically, or excitation of sympathetically, mediated cardiovascular control. Likewise, brain regions that demonstrated decreased activity during the same periods may normally mediate vagal cardiac control or inhibit sympathetic vasomotor function. This highlights the importance of integrating human neuroimaging studies with electrophysiological, stimulation and neuroanatomical tracing experiments in animals for the elucidation of specific parasympathetic *versus* sympathetic pathways between cortical and subcortical structures associated with baroreceptor reflex function.

It is possible that the observed patterns of neural activity measured during the LBNP protocol are related to the central processing of sensory or emotional stimuli. As stated above, we attempted to minimize these confounding influences from those mediating autonomic cardiovascular control by comparing the cortical activity measured during 5-mmHg LBNP to that measured during higher levels of suction. Moreover, the majority of our participants had participated in previous fMRI experiments and a subset of them performed a repeat neuroimaging session in the current study. None of the participants reported any adverse feelings of emotional stress or subjective arousal during the scanning periods.

A recent computed tomography investigation observed a decrease in cerebral blood volume (CBV) without a significant reduction in CBF within cerebral grey matter during LBNP (Wilson *et al.* 2005). Reduced CBV within the postcapillary venous compartment would produce a decrease in the relative concentration of deoxyhaemoglobin (the endogenous contrast agent used in BOLD imaging) and produce an artificial increase to the BOLD signal in affected regions. However, such an effect should manifest itself as global BOLD signal changes throughout the cerebral cortex. To account for global variations in BOLD signal, intensity normalization (i.e. grand mean scaling) was performed to minimize these confounding contributions while still allowing for the detection of relative changes in cerebral metabolic activity.

This normalization procedure, together with the finding of specific, lateralized and reproducible cortical activation patterns correlated with subject-dependent changes in HR and the magnitude of baroreceptor unloading, suggests that the BOLD signal changes reported in this study result from the recruitment of central autonomic centres related to the baroreflex and not from overall changes in cerebral haemodynamics.

Summary

To our knowledge, we have demonstrated for the first time the cortical regions responsible for the modulation of baroreceptor-mediated autonomic cardiovascular function independent of the confounding feedback effects produced by large changes in arterial blood pressure or volitional effort. Both mild and moderate levels of LBNP were associated with increases in MSNA but elevations in HR were only produced with 35-mmHg LBNP. Therefore, we postulate that the neural cortical structures commonly observed during both mild and moderate levels of baroreceptor unloading may be implicated in the control of sympathetically mediated pressor responses (i.e. increases in MSNA) whereas, those cortical regions involved in moderate levels of simulated orthostatic stress may be predominantly responsible for the modulation of cardiac chronotropic control. Specifically, the results suggest that a cortical network involving the right superior posterior insula, the fronto-parietal cortices and the left cerebellum are activated during baroreceptor unloading, to increase HR and MSNA in an attempt to maintain arterial blood pressure homeostasis. Furthermore, the data suggest that brain sites including the bilateral anterior insular cortices, the ACC, orbito-frontal, amygdala, midbrain and mediodorsal nucleus of the thalamus act to suppress sympatho-excitatory activity at rest and that baroreceptor unloading may remove this inhibition.

References

Barberi EA, Gati JS, Rutt BK & Menon RS (2000). A transmit-only/receive-only (TORO) RF system for high-field MRI/MRS applications. *Magn Reson Med* **43**, 284–289.

Bechara A, Tranel D, Damasio H, Adolphs R, Rockland C & Damasio AR (1995). Double dissociation of conditioning and declarative knowledge relative to the amygdala and hippocampus in humans. *Science* **269**, 1115–1118.

Bradley DJ, Ghelarducci B, Paton JF & Spyer KM (1987*a*). The cardiovascular responses elicited from the posterior cerebellar cortex in the anaesthetized and decerebrate rabbit. *J Physiol* **383**, 537–550.

Bradley DJ, Pascoe JP, Paton JF & Spyer KM (1987*b*). Cardiovascular and respiratory responses evoked from the posterior cerebellar cortex and fastigial nucleus in the cat. *J Physiol* **393**, 107–121.

Buchanan SL, Valentine J & Powell DA (1985). Autonomic responses are elicited by electrical stimulation of the medial but not lateral frontal cortex in rabbits. *Behav Brain Res* **18**, 51–62.

Butcher KS & Cechetto DF (1995). Autonomic responses of the insular cortex in hypertensive and normotensive rats. *Am J Physiol* **268**, R214–R222.

Cechetto DF & Calaresu FR (1983). Response of single units in the amygdala to stimulation of buffer nerves in cat. *Am J Physiol* **244**, R646–R651.

Cechetto DF & Calaresu FR (1984). Units in the amygdala responding to activation of carotid baro- and chemoreceptors. *Am J Physiol* **246**, R832–R836.

Cechetto DF & Calaresu FR (1985). Central pathways relaying cardiovascular afferent information to amygdala. *Am J Physiol* **248**, R38–R45.

Cechetto DF & Saper CB (1990). Role of the cerebral cortex in autonomic function. In *Central Regulation of Autonomic Function*, ed. Loewy AD & Spyer KM, pp. 208–223. Oxford University Press, New York.

Chen CH, Williams JL & Lutherer LO (1994). Cerebellar lesions alter autonomic responses to transient isovolaemic changes in arterial pressure in anaesthetized cats. *Clin Auton Res* **4**, 263–272.

Critchley HD, Corfield DR, Chandler MP, Mathias CJ & Dolan RJ (2000). Cerebral correlates of autonomic cardiovascular arousal: a functional neuroimaging investigation in humans. *J Physiol* **523**, 259–270.

Critchley HD, Mathias CJ, Josephs O, O'Doherty J, Zanini S, Dewar BK, Cipolotti L, Shallice T & Dolan RJ (2003). Human cingulate cortex and autonomic control: converging neuroimaging and clinical evidence. *Brain* **126**, 2139–2152.

Critchley HD, Wiens S, Rotshtein P, Ohman A & Dolan RJ (2004). Neural systems supporting interoceptive awareness. *Nat Neurosci* **7**, 189–195.

Dampney RA (1994). Functional organization of central pathways regulating the cardiovascular system. *Physiol Rev* **74**, 323–364.

Delius W, Hagbarth KE, Hongell A & Wallin BG (1972). General characteristics of sympathetic activity in human muscle nerves. *Acta Physiol Scand* **84**, 65–81.

Fagius J & Karhuvaara S (1989). Sympathetic activity and blood pressure increases with bladder distension in humans. *Hypertension* **14**, 511–517.

Fish DR, Gloor P, Quesney FL & Olivier A (1993). Clinical responses to electrical brain stimulation of the temporal and frontal lobes in patients with epilepsy. Pathophysiological implications. *Brain* **116**, 397–414.

Fredrikson M, Furmark T, Olsson MT, Fischer H, Andersson J & Langstrom B (1998). Functional neuroanatomical correlates of electrodermal activity: a positron emission tomographic study. *Psychophysiology* **35**, 179–185.

Gelsema AJ, Agarwal SK & Calaresu FR (1989). Cardiovascular responses and changes in neural activity in the rostral ventrolateral medulla elicited by electrical stimulation of the amygdala of the rat. *J Auton Nerv Syst* **27**, 91–100.

Hagbarth KE & Vallbo AB (1968). Pulse and respiratory grouping of sympathetic impulses in human muscle-nerves. *Acta Physiol Scand* **74**, 96–108.

Halliwill JR, Lawler LA, Eickhoff TJ, Joyner MJ & Mulvagh SL (1998). Reflex responses to regional venous pooling during lower body negative pressure in humans. *J Appl Physiol* **84**, 454–458.

Harper RM, Bandler R, Spriggs D & Alger JR (2000). Lateralized and widespread brain activation during transient blood pressure elevation revealed by magnetic resonance imaging. *J Comp Neurol* **417**, 195–204.

Henderson LA, Macey PM, Macey KE, Frysinger RC, Woo MA, Harper RK, Alger JR, Yan-Go FL & Harper RM (2002). Brain responses associated with the Valsalva maneuver revealed by functional magnetic resonance imaging. *J Neurophysiol* **88**, 3477–3486.

Henderson LA, Richard CA, Macey PM & Runquist ML, Yu PL, Galons JP & Harper RM (2004). Functional magnetic resonance signal changes in neural structures to baroreceptor reflex activation. *J Appl Physiol* **96**, 693–703.

Henderson LA, Woo MA, Macey PM, Macey KE, Frysinger RC, Alger JR, Yan-Go F & Harper RM (2003). Neural responses during Valsalva maneuvers in obstructive sleep apnea syndrome. *J Appl Physiol* **94**, 1063–1074.

Johnson JM, Rowell LB, Niederberger M & Eisman MM (1974). Human splanchnic and forearm vasoconstrictor responses to reductions of right atrial and aortic pressures. *Circ Res* **34**, 515–524.

Kimmerly DS, O'Leary DD & Shoemaker JK (2004). Test-retest repeatability of muscle sympathetic nerve activity: influence of data analysis and head-up tilt. *Auton Neurosci* **114**, 61–71.

Kimmerly DS & Shoemaker JK (2002). Hypovolemia and neurovascular control during orthostatic stress. *Am J Physiol Heart Circ Physiol* **282**, H645–H655.

King AB, Menon RS, Hachinski V & Cechetto DF (1999). Human forebrain activation by visceral stimuli. *J Comp Neurol* **413**, 572–582.

Klassen LM & Menon RS (2004). Robust automated shimming technique using arbitrary mapping acquisition parameters (RASTAMAP). *Magn Reson Med* **51**, 881–887.

Lancaster JL, Woldorff MG, Parsons LM, Liotti M, Freitas CS, Rainey L, Kochunov PV, Nickerson D, Mikiten SA & Fox PT (2000). Automated Talairach atlas labels for functional brain mapping. *Hum Brain Mapp* **10**, 120–131.

Maldjian JA, Laurienti PJ, Kraft RA & Burdette JH (2003). An automated method for neuroanatomic and cytoarchitectonic atlas-based interrogation of fMRI data sets. *Neuroimage* **19**, 1233–1239.

Nisimaru N, Okahara K & Yanai S (1998). Cerebellar control of the cardiovascular responses during postural changes in conscious rabbits. *Neurosci Res* **32**, 267–271.

Oppenheimer SM & Cechetto DF (1990). Cardiac chronotropic organization of the rat insular cortex. *Brain Res* **533**, 66–72.

Oppenheimer SM, Gelb A, Girvin JP & Hachinski VC (1992). Cardiovascular effects of human insular cortex stimulation. *Neurology* **42**, 1727–1732.

Owens NC & Verberne AJ (1996). An electrophysiological study of the medial prefrontal cortical projection to the nucleus of the solitary tract in rat. *Exp Brain Res* **110**, 55–61.

Parati G, Casadei R, Groppelli A, Di Rienzo M & Mancia G (1989). Comparison of finger and intra-arterial blood pressure monitoring at rest and during laboratory testing. *Hypertension* **13**, 647–655.

Polson JW, Potts PD, Li YW & Dampney RA (1995). Fos expression in neurons projecting to the pressor region in the rostral ventrolateral medulla after sustained hypertension in conscious rabbits. *Neuroscience* **67**, 107–123.

Pool JL & Ransohoff J (1949). Autonomic effects on stimulating rostral portion of cingulate gyri in man. *J Neurophysiol* **12**, 385–392.

Soufer R, Bremner JD, Arrighi JA, Cohen I, Zaret BL, Burg MM & Goldman-Rakic P (1998). Cerebral cortical hyperactivation in response to mental stress in patients with coronary artery disease. *Proc Natl Acad Sci U S A* **95**, 6454–6459.

Spyer KM (1999). Central nervous control of the cardiovascular system. In *A Textbook of Clinical Disorders of the Autonomic Nervous System*, ed. Mathias CJ & Bannister R, pp. 45–55. Oxford University Press, Oxford.

Stevens PM & Lamb LE (1965). Effects of lower body negative pressure on the cardiovascular system. *Am J Cardiol* **16**, 506–515.

Taylor JA, Halliwill JR, Brown TE, Hayano J & Eckberg DL (1995). 'Non-hypotensive' hypovolaemia reduces ascending aortic dimensions in humans. *J Physiol* **483**, 289–298.

Terreberry RR & Neafsey EJ (1987). The rat medial frontal cortex projects directly to autonomic regions of the brainstem. *Brain Res Bull* **19**, 639–649.

Tranel D & Damasio H (1994). Neuroanatomical correlates of electrodermal skin conductance responses. *Psychophysiology* **31**, 427–438.

Verberne AJ & Owens NC (1998). Cortical modulation of the cardiovascular system. *Prog Neurobiol* **54**, 149–168.

Weisz J, Emri M, Fent J, Lengyel Z, Marian T, Horvath G, Bogner P, Tron L & Adam G (2001). Right prefrontal activation produced by arterial baroreceptor stimulation: a PET study. *Neuroreport* **12**, 3233–3238.

Williamson JW, McColl R & Mathews D (2004). Changes in regional cerebral blood flow distribution during postexercise hypotension in humans. *J Appl Physiol* **96**, 719–724.

Williamson JW, Nobrega AC, McColl R, Mathews D, Winchester P, Friberg L & Mitchell JH (1997). Activation of the insular cortex during dynamic exercise in humans. *J Physiol* **503**, 277–283.

Wilson TD, Shoemaker JK, Kozak R, Lee TY & Gelb AW (2005). Reflex-mediated reduction in human cerebral blood. *J Cereb Blood Flow Metab* **25**, 136–143.

Yasui Y, Itoh K, Kaneko T, Shigemoto R & Mizuno N (1991). Topographical projections from the cerebral cortex to the nucleus of the solitary tract in the cat. *Exp Brain Res* **85**, 75–84.

Zhang ZH, Dougherty PM & Oppenheimer SM (1999). Monkey insular cortex neurons respond to baroreceptive and somatosensory convergent inputs. *Neuroscience* **94**, 351–360.

Zhang ZH & Oppenheimer SM (1997). Characterization, distribution and lateralization of baroreceptor-related neurons in the rat insular cortex. *Brain Res* **760**, 243–250.

Zhang ZH & Oppenheimer SM (2000*a*). Baroreceptive and somatosensory convergent thalamic neurons project to the posterior insular cortex in the rat. *Brain Res* **861**, 241–256.

Zhang ZH & Oppenheimer SM (2000*b*). Electrophysiological evidence for reciprocal insulo-insular connectivity of baroreceptor-related neurons. *Brain Res* **863**, 25–41.

Zhang ZH, Rashba S & Oppenheimer SM (1998). Insular cortex lesions alter baroreceptor sensitivity in the urethane-anesthetized rat. *Brain Res* **813**, 73–81.

Zoller RP, Mark AL, Abboud FM, Schmid PG & Heistad DD (1972). The role of low pressure baroreceptors in reflex vasoconstrictor responses in man. *J Clin Invest* **51**, 2967–2972.

Acknowledgements

We thank the subjects for their cooperation and also acknowledge the expert technical assistance of Jason Bakker, Nicholas Massé, Savio Wong and Angela Cechetto. This research project was supported by the Ontario March of Dimes, the Canadian Space Agency and the Heart and Stroke Foundations of Ontario (no. NA 5020) and Canada. D.D.O. and D.S.K. were recipients of a Heart and Stroke Foundation of Canada Research Fellowship and Doctoral Research Award, respectively.